ELSEVIER

Ceramics International 32 (2006) 13–19

CERAMICS INTERNATIONAL

www.elsevier.com/locate/ceramint

Wear behavior of alumina–titania coatings: analysis of process and parameters

Sofiane Guessasma [a,*], Mokhtar Bounazef [b], Philippe Nardin [c], Tahar Sahraoui [a]

[a] *LLERMPS—UTBM, Site de Sévenans, 90010 Belfort Cedex, France*
[b] *Hydrology and Materials Laboratory, Sidi Bel Abbe's University, Algeria*
[c] *FEMTO ST—UMR CNRS 6174-CREST, Parc Tech., Belfort, France*

Received 19 July 2004; received in revised form 25 August 2004; accepted 20 November 2004
Available online 17 February 2005

Abstract

The effect of injection parameters of atmospheric plasma spray process is studied on tribological behavior of Al_2O_3–13% TiO_2 plasma sprayed coatings.

The suggested correlations between the process parameters and the friction coefficient were mainly explained by the effect of the process parameters on the in-flight particle characteristics and related to bounding mechanism during coating formation. This work demonstrated experimentally that the knowledge of the particle characteristics before the coating formation is important to predict the wear behavior of the ceramic.

Keywords: Alumina–titania coating; Ceramic; Atmospheric plasma spraying (APS); Wear; Friction coefficient

1. Introduction

Thermal spraying is a technique of coating manufacturing implementing a wide variety of processes and materials. The atmospheric plasma spraying (APS) is one of these processes based on the creation of a plasma jet to melt a feedstock powder. The powder particles are injected with the aid of a carrier gas and gain their velocity and temperature by thermal and kinematic transfers from the plasma jet. At the surface of the part to be covered, such particles flatten and solidify rapidly forming a stacking of lamellas. The coating microstructure is then characterized by a heterogeneous phase configuration with porosity content due to the voids left by the staking process.

Plasma sprayed alumina–titania ceramic is one of the materials largely used in the APS process. It is known for its wear, corrosion, and erosion resistance applications.

Control of ceramic in-service properties and especially wear behavior is sensitive to the large number of the processing parameters and their interdependencies [1]. Energetic and injection parameters are some of these parameter categories. The first category influences plasma jet properties such as enthalpy and velocity and consequently in-flight particle velocity and temperature during their flight [2–4]. The second category controls particle trajectory in the plasma jet [5,6] and has a secondary effect on particle characteristics (i.e., velocity and temperature). Spray process control considers generally the effect of the energetic parameters, which proved to be significant to improve in-flight particle characteristics [4], coating mechanical properties [7,8] and consequently in-service properties. However, few studies consider the effect of injection parameters because of their secondary effect [9]. Marsh et al. [10] reported the decrease of the deposition efficiency with the increase of the powder feed rate. Fisher [11] related this decrease to the decrease of thermal exchanges between the plasma jet and powder particles, which decreases particle temperature [3,12–14]. Fauchais et al. [9] discussed the effect of the injection velocity on the

* Corresponding author. Present address: INRA, B.I.A., Rue de la Géraudière, B.P. 71627, 44316 Nantes Cedex 03, France. Tel.: +33 2 40 67 50 36; fax: +33 2 40 67 51 67.
E-mail address: guessasm@nantes.inra.fr (S. Guessasma).

0272-8842/$30.00
doi:10.1016/j.ceramint.2004.11.014

particle trajectory pointing out the influence on the particle velocity and temperature. Madejeski [15] and McPherson [16] related the in-flight particle temperature and velocity to flattening process and coating cohesion. Other authors discussed the effect of particle velocity on the deposition efficiency [3,14,17], adhesion [17,18] and other properties [4,14,18,19]. Some studies related the process parameters to coating in-service properties such as the wear behavior [20,21]. Wear of ceramics and especially alumina is identified as a complex mechanism in which different stages operate [22]. These are tribochemical reaction, plastic flow, microfracture and glassy surface film. These stages are sensitive to the mechanical properties of the ceramic coating, which, in turn, are dependent on the process parameters.

In such a way, this study aimed at considering the effect of the injection parameters on the wear behavior of Al_2O_3–13% TiO_2 plasma sprayed coatings under different spray parameters. After spraying, sample friction coefficients were determined using a Pin-On-Disk (POD) test.

2. Experimental procedure

2.1. Coating fabrication

A commercially available alumina–titania ceramic powder (METCO[1] #130, Al_2O_3 13 wt.% TiO_2 of +15 −53 μm typical particle size distribution) from Sultzer Metco,[1] was thermally sprayed onto metallic coupons (25 mm in diameter and 10 mm in thickness) under atmospheric plasma spraying conditions. The powder compounds were fused and crushed permitting to obtain an elongated particle shape with a low flowability and a good thermal exchange property (Fig. 1a).

A F4—6 mm gun from Sulzer Metco[1] operating at power levels up to 50 kW was chosen to realize all the experiments. The plasma jet was generated using a gas mixture of argon and hydrogen. The argon gas was used also as a carrier gas for the injection of powder particles. The gun tip was maintained at a spray distance of 125 mm far from the substrate plan. The powder injection was external to the torch and directed perpendicular to the plasma flow and parallel to the torch trajectory. This distance was varied from 6 to 8 mm (Table 1). The feed rate was 22 g min^{-1}. The spray configuration was a combination of a rotating sample holder and a torch uniform and linear scan. These defined the scanning step and velocity parameters, which were fixed. The linear velocity of the sample holder was about 0.84 m s^{-1}. The spray angle was set to 90°. To avoid adhesion problems due different thermal expansion coefficients between the coating and the substrate and limit the stress level, 2 air-cooling jets were added to the spray configuration to lower the coating temperature during deposition (Table 1). These were displaced at 110 mm from the sample holder. The air is supplied from the building air compressor and is controlled by a pressure regulator.

Table 1
The spray conditions

Parameter	Value
Gun	Sulzer-Metco F4
Arc current	530
Argon gas flow rate (SLPM)	40
Hydrogen gas flow rate (SLPM)	14
Argon carrier gas flow rate (SLPM)	2.2, **3.2**, 4.4
Injection distance (mm)	**6**, 7, 8
Feedstock feed rate (g min^{-1})	22
Feedstock injector internal diameter (mm)	1.8
Spray distance (mm)	125
Spray angle (°)	90
Scanning step (mm)	12
Sample holder angular velocity (rpm)	80
Robot scanning velocity (mm s^{-1})	16

The reference condition values were labelled with bold characters.

Experiments were realized considering two process parameters: carrier gas flow rate (V_{CG}) and injection distance (D_{inj}). This last parameter expresses the distance between the injector tip and the torch geometric axis. Each of these parameters was varied with respect to a reference condition to low and high levels as defined in Table 1.

The polishing process necessary to obtain optical micrographs was performed on a fully automatic polishing system (Vanguard from Buehler) to reduce the bias introduced by the operator. Samples were cross-sectioned using the Accutom-5 machine from Struers.[2] Cutting was performed under cooling liquid jet with a rate of 0.8 SLPM. Coating characterization was performed on the cross sections revealing the microstructure shown in Fig. 1.

The obtained coatings exhibit a high morphological and micorstructural anisotropies as shown in Fig. 1. The top view reveals a significant segmentation of the coating due to large solidification rates when the splats built up (Fig. 1a). In addition, the cross section view (Fig. 1b) shows a certain amount of unmolten particles which adhere weakly to the coating and represent the source of wrenching observed when polishing the samples.

2.2. Coating friction and wear behavior characterization

Friction and wear tests were performed using a POD arrangement on a CSEM[3] tribometer. The POD test is a model test for determining friction characteristics and wear behaviors of two solid surfaces being in sliding contact. The test configuration corresponding to a single point contact is

[1] Sulzer-Metco AG, Rigackerstrasse 16, 5160 Wohlen, Switzerland.

[2] Struers Inc., Cleaveland, OH, USA.

[3] CSEM: Centre Suisse d'Electronique et de Microtechnique SA, Jaquet Droz 1, 2007 Neuchâtel, Switzerland.

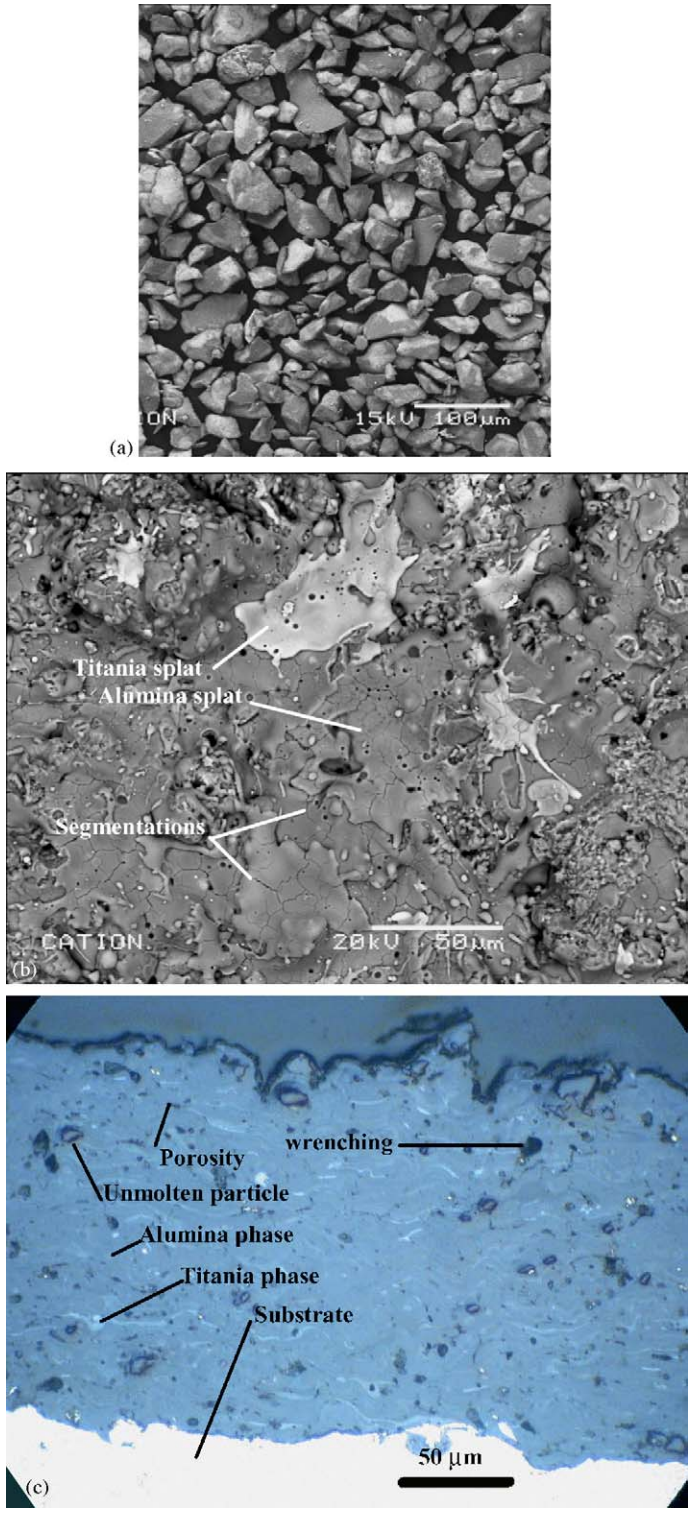

Fig. 1. (a) Particle morphology of the alumina–titania powder. Typical microstructure of alumina–titania coating obtained using reference spray conditions, (b) cross section of the coating revealed by optical microscopy, and (c) micrograph of surface revealed by SEM.

shown in Fig. 2. Before performing the test, samples were ground to lower their surface roughness (i.e., average roughness less than 1 μm) in fact the relationship between roughnesses of the slided materials is crucial to determine the wear process. This is why it has to be lowered enough: as the ball presents a good finishing state, a high roughness may cause a high degradation of the ball material if the coating roughness is large and a negative wear can operate. This wear corresponds to the ball material deposited on the wear track. In addition to this a technical factor limits the

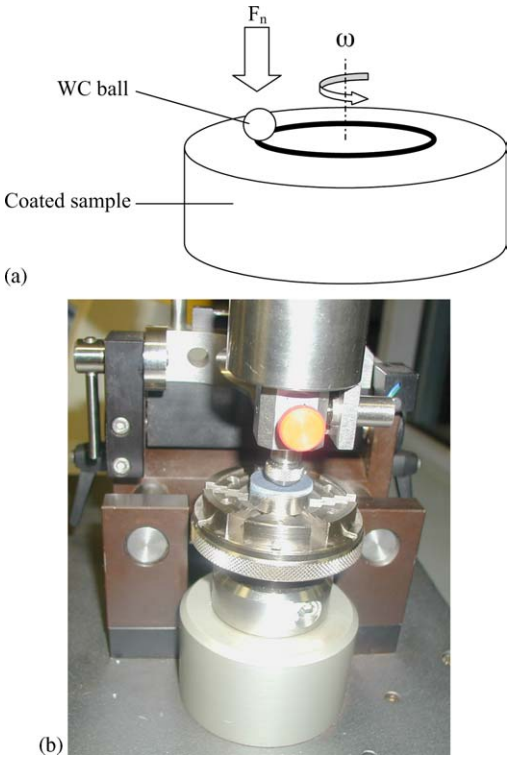

Fig. 2. The POD experiment: ball on disk configuration. $F_n = 5$ N is the applied load and $\omega = 394$ rpm is the angular velocity. (a) Illustration of the principle and (b) a photograph of the setup.

Table 2
POD experiment parameters

Test parameter	Value
Sliding velocity (m s^{-1})	0.33
Applied load (N)	5
Sliding time (s)	3060

roughness of the material to be used when implementing a POD test. In fact, a large roughness causes significant vibrations of the magnetic sensor which can false the estimation of the friction coefficient.

The coated sample was slided against a 6 mm ball made of WC/Co under an applied load of 5 N. The sliding contact was maintained at 6 mm from the sample centre. The sample was rotated at 394 rpm corresponding to a linear speed of 0.33 m s^{-1}. The sliding time was approximately 53 min. The test parameters are summarized in Table 2.

3. Results and discussion

Fig. 3 shows the friction coefficient evolution as function of sliding time. One can distinguish two regions called running-in and stabilization regions [23]. These are related to different wear mechanisms. The first one is related to the running of the materials against themselves and the other one consider the system of the part (i.e., the coating) and the

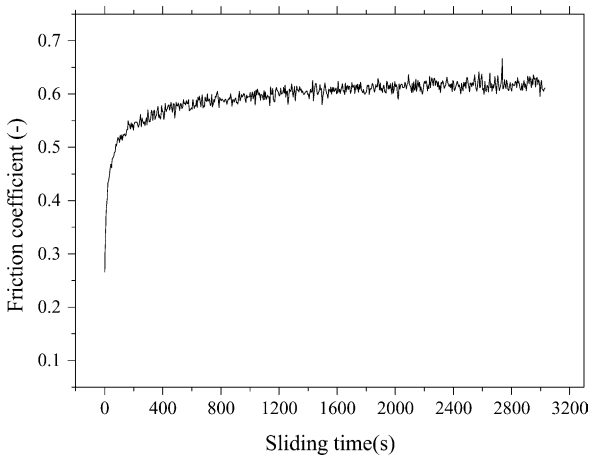

Fig. 3. Evolution of the friction coefficient vs. the sliding time for the system WC/Co—(Al_2O_3–13 wt.% TiO_2) for reference condition ($V_{CG} = 3.2$ SLPM, $D_{inj} = 6$ mm).

counterpart (i.e., the ball). As the roughness of the materials is reduced in the running-in period, the friction coefficient increases because of the contact surface increase. Then, the value of the friction coefficient stabilizes representing the wear behavior of the considered material couple. Fig. 4a shows a top view of the coating after wear process revealed by Laser profilometry. The wear track appears in a clear grey level compared to the rest of the sample. Its width is typically 2 mm. It is remarked that no considerable scuffing is found on the worn surface despite of the fact that friction coefficient was significantly large (Fig. 4b). Thus, the variation of the friction coefficient could be attributed mainly to two factors [24]:

- nonuniform rotation of the motor;
- intrinsic wear behavior in which unmolten particles and porosity play determinant role.

In addition, one can distinguishes the tribofilm formed during sliding as exhibiting a cohesive character (Fig. 4b). Indeed, during the process, particles from mating surfaces are detached and compacted before crushed again in the track. This renders the tribofilm more cohesive [25,26]. The analysis of surface texture reveals that the average roughness in the wear track was 1.1 μm and a maximum roughness of 6.5 μm (Fig. 4c).

The running and stabilization regions were close similar when varying each of the injection parameters (Fig. 5) which demonstrates that friction mechanisms were the same whatever process parameter values. Actually, this is an obvious result as coating phase content did not change significantly. Indeed, injection parameters have a lower effect on alumina and titania evaporations compared to energetic parameters if these are varied in a reasonable range as the case of the spray conditions used in this study. This states also that friction mechanisms were directly related to

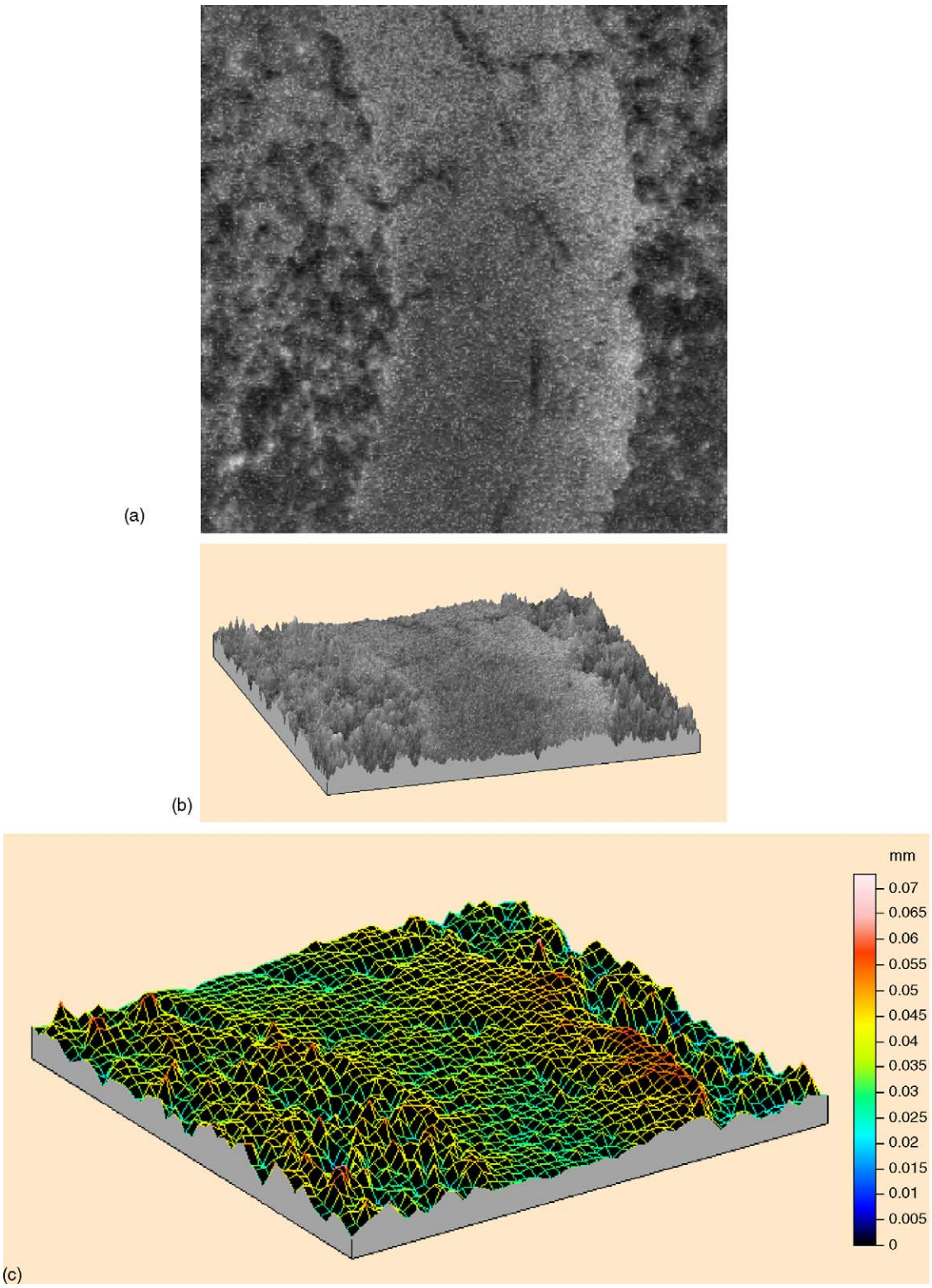

Fig. 4. Laser profilometry trace of wear track generated during the sliding process. (a) Top view, (b) 3-D view and (c) analysis of surface roughness.

bounding mechanisms and porosity level, which are more believed to be sensitive to injection parameters.

Due to the variability of friction coefficient as a consequence to the different wear regimes, calculation of average friction coefficient values was performed using the plot of inverse normal cumulative distribution (Fig. 5b). In this plot, the two regimes are represented by two linear segments clearly identified. The friction

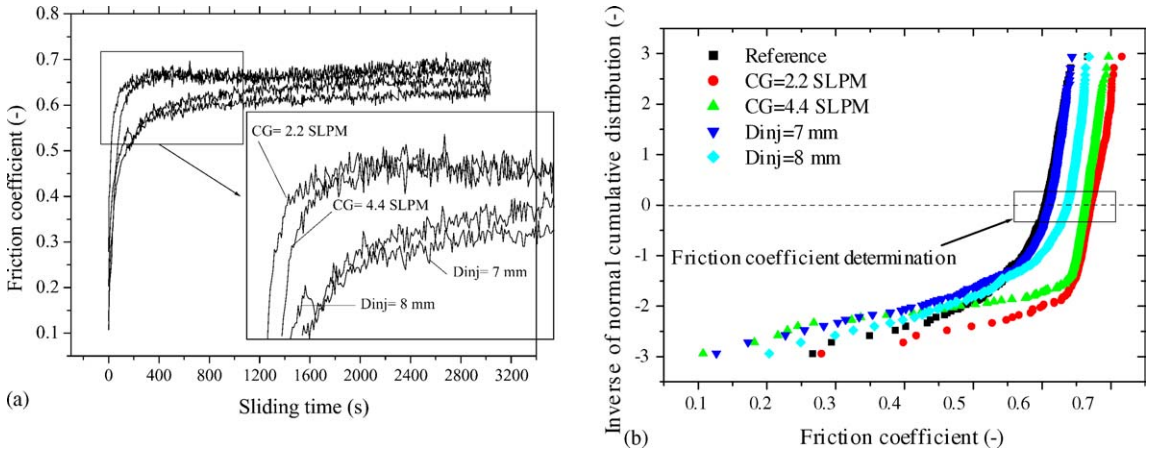

Fig. 5. (a) Evolution of the friction coefficient vs. the sliding time for the system WC/Co—(Al_2O_3–13 wt.% TiO_2) for different injection parameters. (b) Plot of the inverse cumulative distribution for the determination of the friction coefficient.

Table 3
Friction coefficients as function of the APS processing parameters

Experiment	CG (SLPM)	D_{inj} (mm)	Friction coefficient $\mu(-) \pm \sigma(-)$	Variability σ/μ (%)
A1	3.2	6	0.61±0.010	1.7
B1	2.2	6	0.67±0.013	2.0
B2	4.4	6	0.66±0.010	1.5
B9	3.2	7	0.62±0.009	1.5
B10	3.2	8	0.64±0.012	1.9

Carrier gas flow rate (CG); injector stand-off distance (D_{inj}); mean value of the friction coefficient (μ); standard deviation associated with the mean friction coefficient (σ).

coefficient represents the intersection of the abscise axis with the line representing the interpolation of the steady-state segment.

Based on this method, the average and standard deviation of the friction coefficients for the considered experiments were calculated (Table 3).

Values of the friction coefficients varied from 0.61 to 0.67. The associated variability (i.e., the ratio of the mean to the standard deviation) did not exceed 2%. The best wear resistance (i.e., lowest friction coefficient) was obtained with the test A1 corresponding to the reference condition.

Friction coefficient values for low and high carrier gas flow rate levels were significantly higher than that of reference condition. A linear dependence could not be assumed as seen from the bad correlation factor.

$$f(-) = 0.66 - 0.003 \times V_{CG}(\text{SLPM}); \quad R^2 = 0.1 \qquad (1)$$

At this stage, it was not possible to clearly identify the role of carrier gas flow rate. This parameter influences the injection velocity, which in turn depends on injection regime. For high injection velocity, particles cross the plasma jet and decrease spray efficiency. For low regimes, particle velocity is weak and the penetration is rendered difficult because of the plasma jet viscosity. In both cases, wear resistance property could be lowered. However, carrier gas flow rate regime considered in this study is believed to be an intermediate case between the aforementioned limits. Thus, these results were more related to a problem of particle injection stability, which is more difficult to control.

The increase of friction coefficient relative to the increase of the injection distance (test A1, B9, B10) can be described by a linear dependence, as follows

$$f(-) = 0.52 + 0.015 \times D_{inj}\,(\text{mm}); \quad R^2 = 0.98 \qquad (2)$$

This increase can be related to the depth of particle penetration in the plasma jet [11]. In this case, results suggest that when injection distance is the lowest (6 mm), particle residence time in the plasma core region is increased. This improves particle velocity and temperature when impinging the substrate. In fact interlamellar contact is consequently improved [16] and porosity level reduced [3,8]. Some authors associate to the variation of the injection distance, the dispersion of the particle velocity with respect to their size [9]. As small particles are likely to be dispersed especially near injector wall, the increase of the injection distance causes a large amount of them to by-pass the plasma jet. This aspect has the consequence to decrease the deposition efficiency, which influences the coating density and strength.

4. Summary and conclusions

The effect of injection parameters on wear resistance property of alumina–titania coating was studied. Results

show that friction coefficient increased linearly with the increase of injection distance. This was explained by bounding mechanisms related to improvement of particle velocity and temperature before impinging the substrate. However, a non-linear behavior was identified in the case of carrier gas flow rate. It was not possible to clearly explain the effect of this parameter due probably to a problem of particle injection stability, which is difficult to control.

Acknowledgment

LERMPS is a member of the Institut des Traitements de Surface de Franche-Comté (ITSFC, Surface Treatment Institute of Franche-Comté), France.

References

[1] D.A. Gerdman, N.L. Hecht, Arc Plasma Technology in Materials Science, Springer, Vienna, Austria, 1972.
[2] P. Nylén, J. Wigren, J. Idetjärn, L. Pejryd, On-line microstructure and property control of thermal sprayed abrasive coatings, in: C.C. Berndt, K.A. Kohr, E.F. Lugscheider (Eds.), Thermal Spray 2001: New Surfaces for a New Millenium, ASM International, Materials Park, OH, USA, 2001, pp. 1213–1220.
[3] M. Friis, C. Persson, J. Wigren, Influence of particle in-flight characteristics on the microstructure of atmospheric plasma sprayed yttria stabilized ZrO_2, Surf. Coatings Technol. 141 (2001) 115–127.
[4] M. Prystay, P. Gougeon, C. Moreau, Structure of plasma sprayed zircona coatings tailored by controlling the temperature and velocity of the sprayed particles, J. Thermal Spray Technol. 10 (1) (2001) 67–75.
[5] T. Zhang, D.T. Gawne, B. Liu, Computer modelling of the influence of process parameters on the heating and acceleration of particles during plasma spraying, Surf. Coatings Technol. 132 (2000) 233–243.
[6] J.E. Döring, R. Vassen, D. Stöver, The influence of spray parameters on particle properties, in: E. Lugscheider, P.A. Kammer (Eds.), Proceedings of International Thermal Spray Conference and Exposition, DVS-Verlag GmbH, Düsseldorf, Germany, 2002 pp. 440–445.
[7] D.J. Varacalle, H. Herman, G.A. Bancke, W.L. Riggs, Vacuum plasma sprayed alumina–titania coatings, Surf. Coatings Technol. 54 (55) (1992) 19–24.
[8] T.J. Steeper, D.J. Varacalle Jr., G.C. Wilson, W.L. Riggs, A.J. Rotolico, J.E. Nerz, A design of experimental study of plasma sprayed alumina–titania coatings, in: C.C. Berndt (Ed.), Advances in Coatings Technology, ASM International, Materials Park, OH, USA, 1992 pp. 415–420.
[9] P. Fauchais, J.F. Coudert, A. Vardelle, M. Vardelle, A. Grimaud, P. Roumilhac, State of the art for the understanding of the physical phenomena involved in plasma spraying at atmospheric pressure, in: D.L. Houck (Ed.), Thermal Spray: Advances in Coatings Technology, ASM International, Materials Park, OH, USA, 1987, pp. 11–19.
[10] D.R. Marsh, N.E. Weare, D.L. Walker, Process variables in plasma-jet spraying, J. Metals 2 (1961) 473–478.
[11] I.A. Fisher, Variables influencing the characteristics of plasma-sprayed coatings, Int. Metall. Rev. 17 (1972) 117–125.
[12] P. Fauchais, P. Vardelle, M. Vardelle, A. Vardelle, J.F. Coudert, Plasma spraying of ceramic particles in argon–hydrogen D.C. plasma jet: modelling and measurements of particles in-flight correlation with thermophysical properties of sprayed layers, Met. Trans. 20B (1989) 263–276.
[13] P. Proulx, J. Mostaghimi, M.I. Boulos, Plasma-particle interaction effects in induction plasma modelling under dense loading conditions, Int. J. Heat Mass Transfer 28 (1985) 1327–1336.
[14] A. Refke, G. Barbezat, M. Loch, The benefit of an on-line diagnostic system for the optimization of plasma spray devices and parameters, in: C.C. Berndt, K.A. Kohr, E.F. Lugscheider (Eds.), Thermal Spray 2001: New Surfaces for a New Millenium, ASM International, Materials Park, OH, USA, 2001, pp. 765–770.
[15] J. Madejeski, Solidification of droplets on a cold surface, Int. J. Heat Mass Transfer 19 (1976) 1009–1013.
[16] R. McPherson, The relationship between the mechanism of formation, microstructure and properties of plasma sprayed coatings, Thin Solid Film 83 (1981) 297–310.
[17] P. Nylén, J. Wigren, J. Idetjärn, L. Pejryd, On-line microstructure and property control of thermal sprayed abrasive coatings, in: C.C. Berndt, K.A. Kohr, E.F. Lugscheider (Eds.), Thermal Spray 2001: New Surfaces for a New Millenium, ASM International, Materials Park, OH, USA, 2001, pp. 1213–1220.
[18] V.V. Sobolev, J.M. Guilemany, Flattening of droplets and formation of splats in thermal spraying: a review of recent work—Part 2, J. Thermal Spray Technol. 8 (2) (1999) 301–314.
[19] R. McPherson, P. Cheang, Elastic anisotropy of APS alumina coatings and its relationship to microstructure, in: P. Vincenzini (Ed.), High Performance Ceramic Films and Coatings, Elsevier Science Publishers B.V., Lausanne, Switzerland, 1991, pp. 277–290.
[20] W. Lih, S.H. Yang, C.Y. Su, S.C. Huang, I.C. Hsu, M.S. Leu, Effects of process parameters on molten particle speed and surface temperature and the properties of HVOF CrC/NiCr coatings, Surf. Coatings Technol. 133–134 (2000) 54–60.
[21] M. Vijaya Babu, R. Krishna Kumar, O. Prabhakar, N. Gowri Shankar, Simultaneous optimization of flame spraying process parameters for high quality molybdenum coatings using Taguchi methods, Surf. Coatings Technol. 79 (1996) 276–288.
[22] S. Jahanmir, Friction and Wear of Ceramics, Marcel Dekker, USA, 1994.
[23] V. Fervel, B. Normand, H. Liao, C. Coddet, E. Beche, R. Berjoan, Friction and wear mechanisms of thermally sprayed ceramic and cermet coatings, Surf. Coating Technol. 111 (1999) 255–262.
[24] B.X. Liu, Z.J. Zhang, O. Jin, A comparative study of metastable alloy formation by ion mixing and thermal annealing of multilayers in the immiscible Y–Zr system, J. Alloys Compounds 270 (1988) 186–193.
[25] R. Westergård, S. Hogmarkb, Sealing to improve the wear properties of plasma sprayed alumina by electro-deposited Ni, Wear 256 (2004) 1153–1162.
[26] S. Hogmark, M. Olsson, A. Blomberg, Wear mechanisms of advanced ceramic materials, J. Hard Mater. 32 (1992) 153–167.